

ZoeMatrope: A System for Physical Material Design

Leo Miyashita
University of Tokyo

Kota Ishihara
PKSHA Technology Inc.

Yoshihiro Watanabe
University of Tokyo

Masatoshi Ishikawa
University of Tokyo

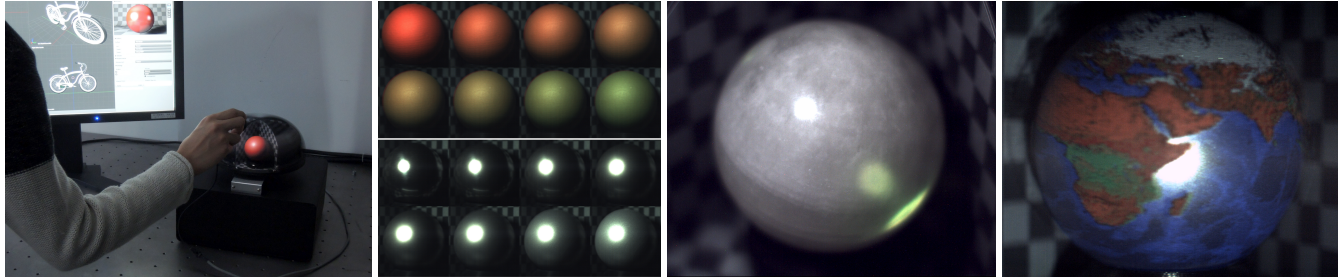


Figure 1: We introduce a novel material display based on a zoetrope and a thaumatrope. (left) The system can represent a variety of realistic materials and assist physical material design. (left center) Material animation. (right center) Augmented material composed of marble and green glass. (right) Spatially-varying material formed by combining many materials.

Abstract

Reality is the most realistic representation. We introduce a material display called ZoeMatrope that can reproduce a variety of materials with high resolution, dynamic range and light field reproducibility by using compositing and animation principles used in a zoetrope and a thaumatrope. With ZoeMatrope, the quality of the material is equivalent to that of real objects and the range of expressible materials is diversified by overlaying a set of base materials in a linear combination. ZoeMatrope is also able to express spatially-varying materials, and even augmented materials such as materials with an alpha channel. In this paper, we propose a method for selecting the optimal material set and determining the weights of the linear combination to reproduce a wide range of target materials properly. We also demonstrate the effectiveness of this approach with the developed system and show the results for various materials.

Keywords: zoetrope, strobe light, thaumatrope, material composition, diffuse, specular

Concepts: •Human-centered computing → Systems and tools for interaction design; •Computing methodologies → Virtual reality; •Hardware → Displays and imagers;

1 Introduction

Realistic materials have recently begun to be rendered in computer graphics. Numerically modeled materials are becoming more and more realistic and are now used even as temporary substitutes for real materials. In the manufacturing and printing industry for instance, computer graphics provides completed images of products,

Permission to make digital or hard copies of all or part of this work for personal or classroom use is granted without fee provided that copies are not made or distributed for profit or commercial advantage and that copies bear this notice and the full citation on the first page. Copyrights for components of this work owned by others than ACM must be honored. Abstracting with credit is permitted. To copy otherwise, or republish, to post on servers or to redistribute to lists, requires prior specific permission and/or a fee. Request permissions from permissions@acm.org. © 2016 ACM.

SIGGRAPH '16 Technical Paper, July 24-28, 2016, Anaheim, CA,
ISBN: 978-1-4503-4279-7/16/07
DOI: <http://dx.doi.org/10.1145/2897824.2925925>

and users can utilize these images for checking whether the materials perform as intended. The realistic presentation of materials is essential for not only designing a material but also confirming the color and gloss in internet shopping. In addition, it enhances various immersive experiences in art, media, and augmented reality.

However, conventional displays cannot represent realistic materials due to their limitations, including resolution, dynamic range and freedom of the viewing and lighting directions. Some research has attempted to improve these issues by using technologies such as projection mapping techniques and specialized displays; however, the results are still far behind reality, or the kinds of expressible materials are limited.

Our key concept to display a realistic material is to use real materials. Display devices using real objects have been developed over a long period of time; the zoetrope and the thaumatrope are two examples of them. The zoetrope is a device that can animate pictures or 3D objects by apparent motion with a rotating base and cut slits or strobe light, as shown in Fig. 2 (a). The thaumatrope is a device that can composite pictures switched at high speed by exploiting persistence of vision, as shown in Fig. 2 (b). In this paper, we propose a visual material display named “ZoeMatrope” which can composite real materials like the thaumatrope and can interactively animate them like the zoetrope as shown in Fig. 2 (c).

The ZoeMatrope system computationally controls timing and intensity of strobe light illumination and expresses protean materials consisting of real materials. For example, when the user sets a red and glossy material on a 3D model on a computer, the ZoeMatrope illuminates only a red object and a glossy object among a number of objects rotating at high speed. As a result, only these two materials are visible, and a composite material that is both red and glossy will be seen in an overlaid manner by the human eye as shown in Fig. 2 (c) left. By setting the timing and intensity of the illumination properly, this system can combine the set of real objects in a linear combination and reproduce or approximate a wide range of material characteristics such as color, roughness or both. Furthermore, by varying the strobe light control, the appearance of the material display can be animated as shown in Fig. 2 (c) right. A real object is the most realistic, and consequently, ZoeMatrope can display materials with outstanding resolution, dynamic range and light field fidelity and will allow the creation of new forms of expression media.

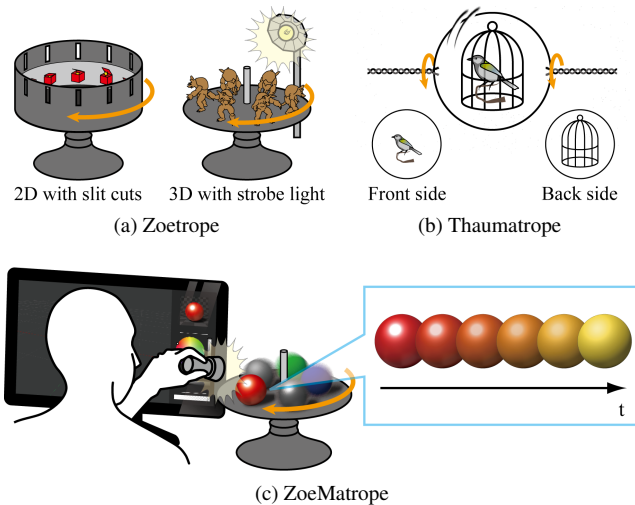


Figure 2: The concept of *ZoeMatrope*. *ZoeMatrope* combines real objects with the principle used in the thaumatrope and animates the material with the principle used in the zoetrope. The objects switched at high speed appear to the human eye to be overlaid and present the realistic material.

On the other hand, since our system is based on time-multiplexing technique, there are some limitations on rigorous reproduction of concave and refractive objects, continuous variations of some parameters including IOR, and ambient light. The effects of these limitations are also analyzed in this paper.

Our specific technical contributions are as follows:

- We propose the *ZoeMatrope* system which can interactively display a wide variety of realistic materials. This system uses real objects as the bases of composition and animation and consequently can achieve outstanding resolution, dynamic range, and light field reproduction. We also introduce a lighting control method for displaying the composite material properly.
- We constructed a mathematical framework for the optimal material selection method. This framework is capable of representing a wide range of materials with a small number of base materials and can be applied to various characteristics of a material.
- We demonstrate the presentation and animation of composite materials, including diffuse, specular, spatially-varying and augmented materials, with the developed system. We also evaluated the expressible range and accuracy of the composite materials.

2 Related Work

Making a catalog of material samples is the most primitive method of checking materials, but this requires an enormous number of samples and it is difficult, in terms of the time and space required, to prepare and cover multifarious materials.

In order to reproduce various materials, past studies have proposed methods using projection mapping techniques or specialized displays [Hullin et al. 2013]. Raskar et al. projected rendered images onto a real object to artificially replace the material properties [2001]. With this method, the target is a real object, and so the

geometrical resolution is the highest possible. Additionally, since the virtual viewpoint and light source characteristics can be controlled, the light field can be simulated with techniques including head tracking. Nayar et al. developed a display that modifies its content according to incident 4D illumination field and can mimic material properties [2004].

As well as these systems, which imitate the viewing and lighting direction for a specific user, recently, display devices that can construct multi-aspect light fields have also been proposed. Jones et al. presented a light field display using a spinning mirror and a projector array system that can display autostereoscopic 3D objects [2007; 2014]. In addition, Glasner et al. presented a display that passively reacts to the illumination and viewpoint without the need for high-cost rendering [2014]. Nevertheless, the image resolution and dynamic range depend on the projector or the display, and the reproducibility of the light field basically does not reach that of reality.

On the other hand, some systems actually control the bidirectional reflectance distribution function (BRDF) by using a deformable screen that can adopt a wavy surface shape. Hullin et al. displayed the BRDF with a ruffled liquid surface [2011], and similarly, Ochiai et al. utilized a liquid film vibrated by ultrasonic waves [2012]. The methods using a waving screen are capable of high resolution and high dynamic range with a natural viewing point and lighting point dependencies for uniform BRDF; however, they have difficulty in reproducing spatially-varying materials and completely dissimilar materials, such as an object with different transparencies. Additionally, the display surface is restricted to a plane. These problems are derived from the reproduction method, which depends on the dynamics and physical properties of fluid. In our system, the appearance of a material depends on control of the light source, and so it is possible to reproduce detailed, spatially-varying materials by using a light source with spatially-varying intensity pattern. Moreover, the reproduction method, which combines real objects, can easily change the expressible materials and the shape of the displayed objects.

Besides, some zoetrope- or thaumatrope-style displays using real objects have been presented. Smoot et al. adaptively controlled the zoetrope strobe illumination and animated a talking character according to human speech in real time [2010]. Ochiai et al. rotated disks and gave a glimpse of interesting expression with a thaumatrope-style display [2011]. Although these state-of-the-art zoetrope- and thaumatrope-style displays provide entertaining images for the human eye, a computational control technique that deals with the effects of both composition and animation has not been proposed. In this paper, we focus on the presentation and animation of a realistic material and propose a novel display system that is computationally controlled based on the optimal illumination strategy to reproduce the target materials.

The proposed method differs from the conventional systems in that our system can express various kinds of materials, including ordinary diffuse, glossy, transparent, velvety, subsurface-scattering, spatially-varying and augmented materials, by preparing only a few real objects. Moreover the method enables realistic material presentation with high resolution, a large dynamic range and high light field fidelity due to the use of real objects.

3 Principles and Hardware System

3.1 Principles of *ZoeMatrope*

Like many zoetropes, *ZoeMatrope* is composed of turntable and strobe light as shown in Fig. 3. The turntable on which some real

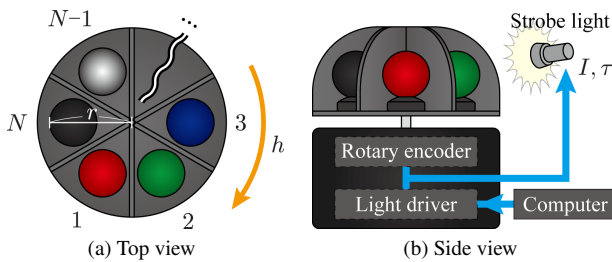


Figure 3: System overview. To overlay the base materials at a specific location, the system requires high-precision alignment and emission timing.

objects (called base materials hereafter) are mounted is fixed to a motor shaft and rotated at high speed. A rotary encoder behind the turntable triggers the strobe light and it irradiates base materials at the proper timing and intensity. By controlling the intensity ratio as shown in Fig. 4, our system can express and animate a variety of composite materials.

The compositing principle is known as afterimages or persistence of vision, and the thaumatrope used this effect to show an overlaid image of two pictures in the 19th century. The temporal resolution of the human eye, called the critical flicker fusion (CFF) rate is said to be about 15 [Hz] with low-intensity light and 60 [Hz] with high-intensity light [Hecht and Smith 1936], and by switching the images faster than the CFF rate, they can be observed as an overlaid image by the human eye. In our system, because the base materials are illuminated at certain locations and appear to be switched without noticeable transitions, a composite material is observed by the user if the switching rate is faster than the CFF rate.

With this compositing principle, the proposed system can combine base materials to express a great variety of realistic materials. However, it should be mentioned that this principle cannot accurately reproduce concave and refractive objects. In the simplified case with a concave object as shown in Fig. 5, the target material is supposed to be compounded with base materials A and B. The composite material can reproduce the light beam path of direct reflection (a) and (b) and multiple reflection (aa) and (bb); however, the base materials A and B cannot exist at the same time and at the same position. Consequently, the result of composition does not include the light transport (ab) and (ba) which passed through both materials A and B. Due to this, the representation including color bleeding can be inaccurate. Similarly, the principle has the same problem in refractive objects and cannot reproduce a strictly accurate appearance. The influence of the limitations is mentioned and visualized in the subsection 5.5. In this paper, we mainly use spherical base materials because it hardly causes any self multiple reflections. Moreover, a sphere is usually used for checking materials because it covers all possible normal directions.

Besides, the animation principle that we adopt is known as apparent motion. The zoetrope used this effect to show moving pictures in the 19th century, and moving 3D figures in recent years. This effect occurs by switching images even at a lower rate than the CFF rate. Based on this principle, our system also animates the material by gradually changing the combination ratios of the base materials.

3.2 Turntable

In our system, the base materials on the turntable are partitioned to reduce influence from other base materials as shown in Fig. 3 and the number of base materials N determines the range of material

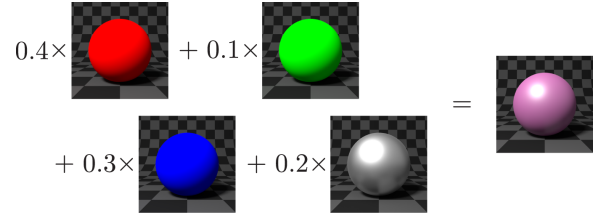


Figure 4: A diagram of the material composition. The composite material is described as a linear combination of base materials. The weights of the summation correspond to the quantities of light radiated onto the individual base materials.

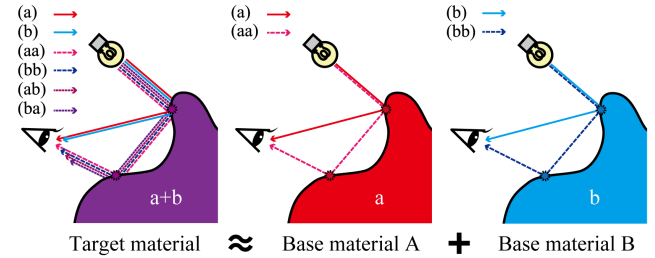


Figure 5: The light beam paths which can be reproduced with the composition principle. The system cannot exactly reproduce multiple reflections. The paths (ab) and (ba) represent reflected light that passes through multiple material components.

gamut. A turntable with a large radius can accommodate many base materials and provide wide gamut; however, we have to consider the trade-off between N and temporal restriction for strobe light.

The longer the strobe light illuminates the rotating objects, the more motion blur occurs, which deteriorates the image quality. Hence, the system should suppress the speed of the objects and illuminate them in as short a time as possible. The resolution of the human eye is said to be about 0.7 ['] [Blackwell 1946], which corresponds to 40.7 [μm] at a distance of 0.2 [m]. Therefore, the blur amount should be suppressed to 40.7 [μm] or below if the closest observation distance is assumed to be 0.2 [m].

Because of this, the distance from the rotation center to the furthest point on the base material, r [m], and the rotation speed, h [Hz] will be important values in the design phase since they determine the maximum emission time, τ_{max} [s], to reduce the amount of blur below a certain value, ϵ [m]. This constraint is written as follows:

$$\tau_{max} = \frac{\epsilon}{2\pi rh}. \quad (1)$$

3.3 Strobe Light

In the proposed system, the appearance of the material depends on the light, and the control of the strobe light has to be performed accurately based on the quantity of light, q [$\text{l}\text{x} \cdot \text{s}$], which is given by

$$q = I\tau \quad (2)$$

Here, I [lx] is the light intensity, and τ [s] is the emission time. The ratio of q emitted to each base material for one cycle determines the blending ratio. A composite material formed with the same quantities of light expresses the same material; however, a shorter emission time should be used to realize a blurless image. The details of the method of determining q of each base material and the method of selecting the base materials to compound a wide range

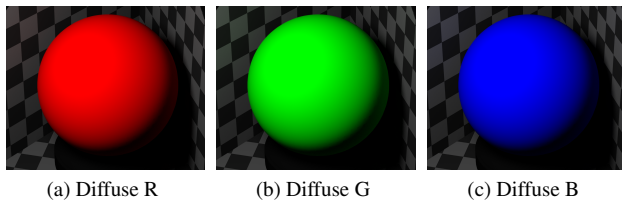


Figure 6: The ideal base materials for achieving color composition.

of materials are described in the next section. In this subsection, we describe the available forms of light source in the *ZoeMatrope*.

When the presented material is not spatially varying, the system does not have to care about the position of the viewpoint and light source since the real world automatically renders the image with perfect viewpoint and light source dependencies. In theory, not only point light sources, but also line, surface and environmental light sources can be used as the light source so long as the quantity of light can be modulated. Additionally, by using a light source with a spatially-varying intensity pattern such as a floodlight with a mask pattern or a projector, the presentation of a spatially-varying material can be realized. Although high temporal resolution is required for the light source, LEDs have sufficient responsiveness, and high-speed projectors that have been developed in recent years [Watanabe et al. 2015] can also be adopted. In the case of a spatially-varying material, calibration of the relative position and attitude of the light source and the base material is required in advance, and the system has to track and align the light source when it moves. However, the proposed system will enable high-quality display of spatially-varying materials because all points on the surface can be controlled independently, and each point is expressed by compounding real objects, as in the case of a uniform material. Besides, a spatially-varying material illuminated with a non-point light source can be simulated by using the light source like a projector array.

4 Material Composition

In this section, we introduce the method of selecting the base material and the method of determining the quantity of light through BRDF composition example. In this example, we assume that the reflection follows the dichromatic reflection model and discuss the proposed methods by dividing the parameters into diffuse color and specular roughness. A later subsection then describes the parameters applicable to the proposed mathematical frameworks and the range of materials that can be combined and animated.

4.1 Diffuse Color Composition

This subsection summarizes the composition method used for realizing a diffuse color. It is well-known that the composition of three primary colors of red, green and blue (RGB) is enough to reproduce various colors. In other words, the color can be expressed by a linear combination of RGB base vectors. Therefore, the composition of RGB base materials indicated in Fig. 6 is sufficient for the human eye to reproduce a diffuse color, and quantities of light for each diffuse color base material, q_R , q_G , and q_B , have only to be set to the RGB ratio, and their sum to the required brightness. On the contrary, when a dark color is compounded, the total quantities of light per cycle should be held constant to avoid changing the brightness of the background as shown in Fig. 7 (a). Light-absorbing object meets this demand, as indicated in Fig. 7 (b) and

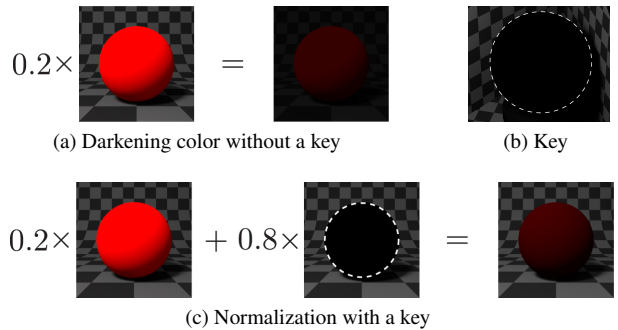


Figure 7: Normalization by a key material. To display a dark color, it is necessary to normalize the quantity of light. A light absorbing material called a key material meets this requirement.

(c). We call this nonreflective object a key (K) material, and the quantity of light received by the key material is represented as q_K in this paper. Eventually, RGBK base materials are required for diffuse color composition, and the quantities of light for the diffuse color base materials are determined by:

$$q_R = R \cdot q_{max}, \quad q_G = G \cdot q_{max}, \quad q_B = B \cdot q_{max} \quad (3)$$

$$q_K = q_{cycle} - (q_R + q_G + q_B). \quad (4)$$

In the above equation, R , G and B refer to the RGB values of the target diffuse color, which take values between 0 and 1, and q_{max} is the product of the maximum intensity of the light source I_{max} and τ_{max} . In addition, q_{cycle} means the target amount of the quantity of light available for one cycle of the turntable. We have to note that the equation (4) shall not apply to the case in which other kinds of base materials are added to the system, but in any case, q_K is defined as the difference between q_{cycle} and the total quantity of light received by the base materials other than the key.

4.2 Specular Roughness Composition

In this subsection, we focus on the composition of the isotropic specular roughness and assume neutral interface reflection (NIR). However, the composition of anisotropic reflection in a certain direction will be realized in the same manner, and a material without the NIR assumption can also be artificially simulated by preparing materials that have RGB specular color, like the composition of the diffuse color, or by switching the color of the light source to the target specular color when the specular base materials are illuminated.

Unlike the color, the spreading shape of the specular reflection generally cannot be separated into certain bases. Then, there are two problems in the composition of specular reflection. The first problem is how to select the set of base materials from existing objects in the real world, and the linear combination of the selected materials has to approximate as wide a range of roughnesses as possible. The second problem is how to determine the quantities of light, that is, the weights of the linear combination, when the set of base materials and the target material are given. In this subsection, we introduce the related work on these two problems and propose a formulation that solves them simultaneously and finds the global optimum.

Because the system approximates the target materials with the positive weighted sum of real objects, some research cannot be applied to the first problem due to negative weights, multiplication or implausible bases. As a selection method that is applicable to real

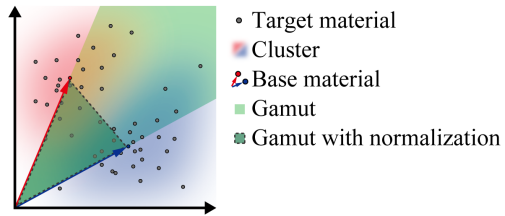


Figure 8: The gamut with the bases determined by a clustering method. In order to reproduce a wide variety of materials, the base materials have to be determined so as to include as many target materials as possible. However, the gamut spanned by the base materials determined by a clustering method is not necessarily optimum. The materials need to be described in much higher dimensions, but the figure above explains them in 2D space without loss of generality.

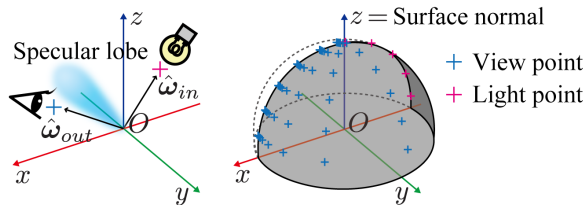


Figure 9: The positions of the viewpoint and light sampling point. In this example, we use an isotropic model, and so we set the sampling points on half of the celestial sphere, in particular, in the specular reflection direction. The viewpoint and light source positions, $\hat{\omega}_{in}$ and $\hat{\omega}_{out}$, in this figure are described by: $\hat{\omega}_{in} = (\cos \theta, 0, \sin \theta)$ with $\theta = \pi(2u + 7)/18$, ($u = 1, 2, \dots, 5$). $\hat{\omega}_{out} = (\sin \phi \cos \psi, \sin \phi \sin \psi, \cos \phi)$ with $\phi = \pi v_\phi/12$, ($v_\phi = 1, 2, \dots, 6$), $\psi = 180^{v_\psi/8-1}\pi$, ($v_\psi = 0, 1, \dots, 7$).

objects as the bases, Kautz et al. proposed the greedy technique [2000] and Ren et al. selected the bases from a BRDF database with a k -nearest neighbor graph [2011]. The greedy algorithm can find a moderate base material, but it is not guaranteed to find the optimum. The clustering method can also find a moderate solution, but this approach is not suitable for including as many materials as possible in the gamut spanned by the base materials, as shown in Fig. 8.

Moreover, to address the second problem, previous approaches introduced the sum of L^1 or L^2 distances between the target specular lobe and an approximation as the definition of the error and succeeded in minimizing the error with an optimization technique [Matusik et al. 2009][Ren et al. 2011].

In the previous approaches, two problems are solved separately but they should be solved as a single problem because the set of the bases cannot be evaluated before the optimal weights are found. In this paper, we aim to define an explicit objective function to evaluate the validity of the base materials and solve these problems simultaneously by discretizing the roughness parameter and introducing a mixed integer linear programming (MILP) problem. Using this MILP, we can obtain the optimal subset of target materials as bases which can reproduce each target material well when they are composited with appropriate weights. The following is the

description of the MILP.

$$\text{Minimize : } \sum_{i,k} e_k^{(i)} \quad (5)$$

$$\text{s.t. } \sum_j x_j \leq n \quad (6)$$

$$\sum_j w_j^{(i)} \leq 1 \quad \text{for all } i \quad (7)$$

$$0 \leq w_j^{(i)} \leq x_j \quad \text{for all } i, j \quad (8)$$

$$e_k^{(i)} \geq + \left(f_k^{(i)} - \sum_j w_j^{(i)} f_k^{(j)} \right) \quad \text{for all } i, k \quad (9)$$

$$e_k^{(i)} \geq - \left(f_k^{(i)} - \sum_j w_j^{(i)} f_k^{(j)} \right) \quad \text{for all } i, k \quad (10)$$

In the above formulation, a specular BRDF is represented as a vector $\mathbf{f} = (f_1, f_2, \dots, f_k, \dots, f_M)$ which is composed of M samples of radiance for different incident direction $\hat{\omega}_{in}$ and viewing direction $\hat{\omega}_{out}$. The target BRDF is a known set whose elements are BRDFs with different discretized roughness m_i and represented as $\mathbf{f}^{(i)}$. The base BRDF is an unknown subset of the target BRDF and represented as $\mathbf{f}^{(j)}$. The weight of $\mathbf{f}^{(j)}$ for $\mathbf{f}^{(i)}$ approximation is also unknown and represented as $w_j^{(i)}$. This optimization evaluates the base material set based on the minimum sum of error between each target and the optimal linear combination of the bases. The error for each radiance f_k is denoted by $e_k^{(i)}$, and it is equal to L1 norm $|f_k^{(i)} - \sum_j w_j^{(i)} f_k^{(j)}|$ after minimization due to constraints (9, 10). Here, binary variable $x_j \in \{0, 1\}$ indicates whether or not the base candidate $\mathbf{f}^{(j)}$ is adopted as the base material; $x_j = 1$ means $\mathbf{f}^{(j)}$ is adopted and $x_j = 0$ means $\mathbf{f}^{(j)}$ is rejected. Equation (6) restricts the number of base materials to n . The sum of weights of base materials to reproduce a target material is bounded by constraint (7). Equation (8) limits the weight of rejected base candidates to 0. This problem is a MILP problem so it can be solved by a general linear programming solver, and the solution which represents n bases and the weights for the target set is guaranteed to be a global optimum when the optimization is done.

This formulation is applicable to any NDF. In this paper, we used GGX NDF [Walter et al. 2007] which is one of the representative NDFs for specular reflection, and searched for the three optimal base materials, like RGB in the case of color. We used $M = 240$ reflectance samples at various $\hat{\omega}_{in}$ and $\hat{\omega}_{out}$, as shown in Fig. 9. We also assumed that stainless steel objects with an index of refraction (IOR) of 2.4 are prepared as the base materials, and the roughness parameter m varies in steps of 0.01, $m \in \{0.00, 0.01, \dots, 1.00\}$. The global optimum was found in about 21 hours with mathematical programming solver Gurobi 6.5, Intel i7-4650U 1.7[GHz] CPU and 8[GB] memory, and GGX NDFs with $m = 0.06, 0.19$, and 0.53 shown in Fig. 10 are found as the optima. The figures also show their optimal weights and the amount of error against the target roughness, as well as the difference in appearance in the second-worst case. The worst case is the approximation for $m = 0.0$, but this is simply the difference between $m = 0.0$ and one of the bases $m = 0.06$ without composition, and so in this paper we indicate the case at the second peak in the error curve where the system generates the target by combining multiple base materials. The proposed method can also manage requests to perfectly reproduce a perfect mirror surface by adding the constraint $x_0 = 1$. In this case, we found the solution $m = 0.00, 0.09$, and 0.39; this combination of base materials can reproduce a perfect mirror, though the sum of error is 22.7 [%] higher than in the optimum case. We also invest-

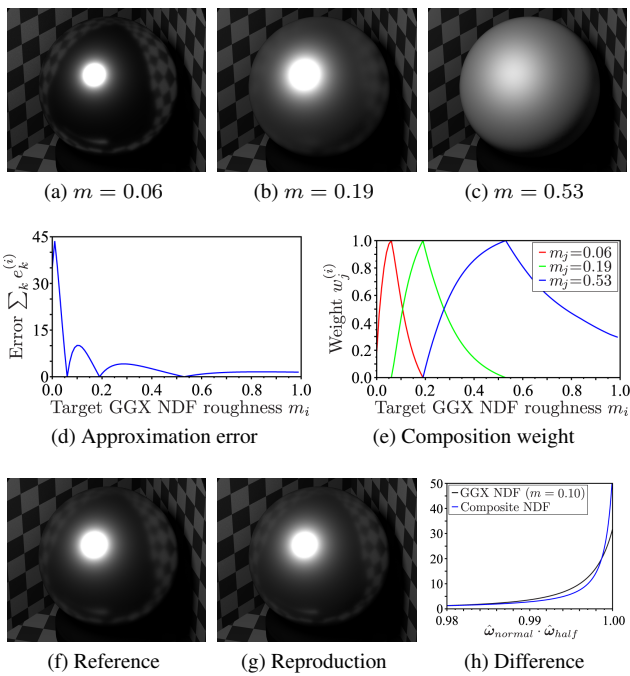


Figure 10: The ideal base materials for the roughness composition. The error for $m = 0.10$ is the maximum of all compositions using multiple materials. The weights used to reproduce the target roughness with a few base materials are optimized and will be the global optimum. Here, $\hat{\omega}_{\text{normal}}$ and $\hat{\omega}_{\text{half}}$ are the normal direction and the half direction for reflection respectively.

tigated the case with a formulation that defines the objective function as the maximum error or sum of squared error; however, this approach showed poor performance in that the objective functions have too high importance on specular materials with small m_i , and the approximation clearly does not follow the target BRDF when m_i increases by even a small amount.

Eventually, it was found that the base materials shown in Fig. 10 are required for the composition of the roughness, and the quantity of light for the base material with m_j in the approximation of m_i is determined by the following; however, almost all weights are zero because only n adopted base materials are able to have a non-zero value.

$$q_j^{(i)} = w_j^{(i)} q_{\max} \quad (11)$$

Just as with the composition of the diffuse color, the total quantity of light q_{cycle} can be normalized with respect to the key material. Besides, in the case of reproducing a material having both diffuse and specular reflections, it can be achieved just by illuminating each base material with the corresponding quantity of light. However, the following redistribution will be necessary to maintain the energy of the reflected light.

$$q_{\text{cycle}} = \alpha(q_R + q_G + q_B) + \beta \sum_j q_j^{(i)} + q_K \quad (12)$$

$$\alpha > 0, \quad \beta > 0, \quad \alpha + \beta = 1 \quad (13)$$

Here, α and β refer to the ratio of the diffuse reflection and specular reflection. Moreover, the total quantity of light, q_{cycle} , and the ratio are similarly maintained by the redistribution when other base materials are compounded.

4.3 The Composition of Other Parameters

In addition to the composition of diffuse and specular reflection, the proposed system can represent various materials, including transparent, translucent, velvety, subsurface scattering, and retroreflective materials and a mixture of them. This flexibility is the advantage of our display system using the composition principle. In this subsection, we discuss a framework for the composition of other materials, and mention the controllable parameters and the limitations of the method.

In the real world, there are many kinds of materials and various parameters which describe the characteristics of these materials. However, some parameters are common among the materials, and these can be handled with the base material selection and composition method proposed in the preceding subsection. Below, we will give three examples: color, roughness, and IOR.

First, we describe the color parameter, which is a common parameter in most materials. The color parameter can be separated into three bases, RGB, and the composition of the color is easily accomplished. The summation weights for the bases should simply be the ratios of RGB, as mentioned in subsection 4.1. In consequence, the color of many materials, including transparent color, can be controlled in the ZoeMatrope system.

Second, we describe the roughness parameter. Besides the specular surfaces described in the preceding subsection, diffuse, transparent, translucent, velvety, and subsurface-scattering materials have a similar parameter to the roughness, although it may be called sharpness, glossiness, deviation or sigma, and so on. For this parameter, the framework of the MILP problem proposed in the preceding subsection can be used. For instance, transparent materials such as glass and acrylic resin have a roughness parameter in the GGX model [Walter et al. 2007], and the optimal bases and weights for the roughness approximation can be found by solving the MILP problem in which BRDF is replaced with a bidirectional transmittance distribution function (BTDF). Similarly, the roughnesses of the other materials can be approximated in the ZoeMatrope system. Refer to Supplemental Material for more information about the optimal bases for other materials.

In contrast, material display systems, including ZoeMatrope and other conventional ones, have difficulty in simulating the IOR. Figure 11 shows the apparent difference in the image in the case of IOR composition of a transparent material. This difficulty originates from the fact that the refraction distorts the image. The composition is the operation of overlaying the images, and so spatial misalignment will occur when an image is distorted. This problem cannot be avoided as long as the system uses the composition principle based on afterimages, and this is one limitation of ZoeMatrope. Nevertheless, the proposed display enables a greater variety of materials to be represented, and the base selection method will enhance the realistic appearance.

4.4 Augmented Materials

The proposed system is also able to represent augmented materials, such as a mixture of diffuse and transparent materials, translucent media compounded with air, and a material that depends on the light source, as shown in Fig. 12. We describe the composition of these three augmented materials, called heterogeneous composition, alpha composition, and light-source-dependent material, in this paper.

Heterogeneous composition refers to a mixture which is extremely difficult to make in the real world, such as a composition of glass, velvet and subsurface scattering. On a computer, there is no dif-

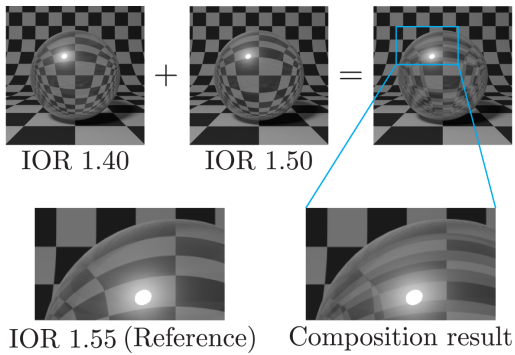


Figure 11: Misalignment in IOR composition. It is difficult for the composition principle to composite parameters related to image distortion.



Figure 12: Augmented materials. Left to right: examples of heterogeneous composition, alpha composition, and light-source-dependent material.

ferent scheme from the composition of diffuse and specular reflections, but presentation with real objects has not been performed. Additionally, alpha composition, which can be enabled by composition of the base materials and empty space, can also be performed in the real world with ZoeMatrope. The alpha composition in the proposed system involves overlaying a base material on air, and so it looks like a translucent medium having an IOR of 1.0, although it is different from general alpha blending in that a backface of the base object will not be visible.

ZoeMatrope also provides materials whose appearance depends on the light source. Since the appearance of the material depends on the control of the strobe light in the proposed system, an augmented material that looks glossy red with light A but matt blue with light B, for example, can be expressed if there are multiple light sources and they are controlled by different schemes.

4.5 Spatially-Varying Material

In the preceding subsections, we described the presentation of a uniform surface with a single composite material; however, the presentation of a spatially-varying material is also desired for assessing the appearance and the expression media.

With the ZoeMatrope system, this is realized by using light having a spatially-varying intensity pattern, including patterned light and light from a projector. In the same way as the light-dependent material mentioned in the preceding subsection, the spatially-varying material utilizes the fact that the appearance is determined by the light source in ZoeMatrope. With projection mapping techniques, an atlas of the quantity of light is mapped to each corresponding point of the base material, and the spatially-varying material is reproduced. The system should track the base material if the light source will move, but all materials mentioned in the preceding subsections can be applied to each point on the surface.



Figure 13: The prototype ZoeMatrope.

5 Implementation and Results

5.1 System Implementation

In this section, we will show the results which were displayed by developed ZoeMatrope prototype. The materials in the figures are photographs, unless otherwise stated. Figure 13 shows the prototype ZoeMatrope system. In this prototype, to shorten the radius of rotation and suppress the object speed, the number of base materials N is 6, and they are arranged to form a hexagonal close-packed structure surrounding the rotation center. For the case where another base material is required to form the target material, the system was designed to replace the base material easily; however, the prototype cannot form more than six base materials at the same time. More bases will reduce the approximation error and make the gamut wider although it makes the rotation radius larger and illumination timing more severe.

The prototype was designed for desktop material display and we set the size of the base materials and the system as around 50 [mm] in diameter, 280 × 250 × 250 [mm] respectively. The system has the following specifications: $r = 87$ [mm], $h = 0 \sim 67$ [Hz] and τ_{max} is about 1.24 [μ s] when h and ϵ are set to 60 [Hz] and 40.7 [μ m], respectively. In consequence, microsecond-order high-speed control of the strobe light is required. In the prototype system, a high-speed LED driver circuit is built in to the system, enabling extremely short-time emission, $\tau = 0 \sim 1000$ [μ s] in units of 1 [μ s]. With 1 [μ s] emission, the prototype system can suppress the blur to 32.8 [μ m] or below at 60 [Hz] and this is small enough for the human eye. Moreover, it can control the intensity of light in an analog fashion with 512 steps, and so the system can adjust the quantity of light sufficiently. The short-time exposure causes a decrease in the maximum light quantity q_{max} . In contrast, the strobe light can maintain sufficient brightness because the LED can be overdriven with a higher voltage than the steady lighting voltage in the case of pulse lighting and provides $I_{max} = 1500$ [lx] at a distance of 200 [mm] in the prototype. The system also has a rotary encoder, which triggers the strobe light and updating of the quantity of light on an external computer. On the computer, the appropriate quantity of light for the target material is computed, and the light-emission settings are updated for the next base material coming around. By updating the set of light quantities, the presented material can be changed in every cycle and animated at h [Hz], as shown in the upper rows in Fig. 14.

We also prepared spherical balls as the base materials, as mentioned in subsection 3.1. The resolution, dynamic range, and light field reproducibility of the system are guaranteed to be optimal due to the use of real objects. The lowest row in Fig. 14 shows the light position dependency, similar to ordinary objects in reality. However, we note that misalignment in the composition can occur depending on the accuracy of the base material installation and circuits, even if the exposure time is short enough. In the following subsection,

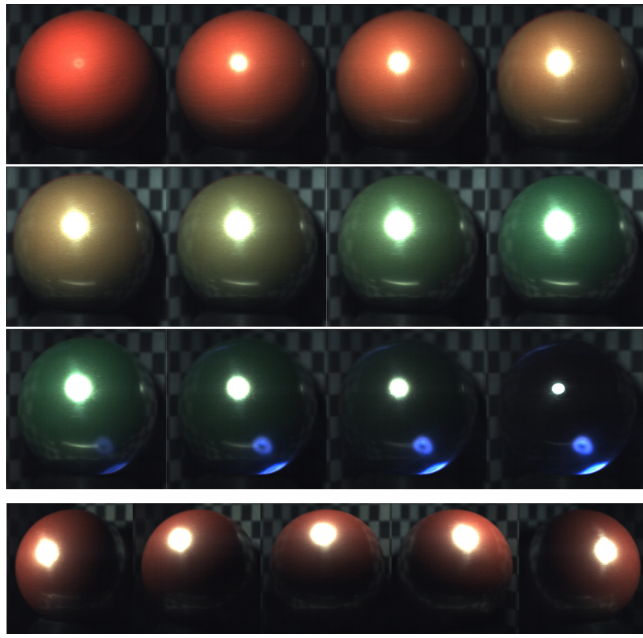


Figure 14: Material composition and animation. The proposed system can change the material either instantaneously or gradually, and the resolution, dynamic range, and dependency on the viewing and lighting directions of the presented object are the same as those of a real object.

we will evaluate the expression ability of the *ZoeMatrope*.

5.2 Color Reproduction Gamut

In order to evaluate the composition of the color, we prepared diffuse and transparent RGB base materials as shown in Fig. 15 (a) ~ (f). Ideally, the diffuse bases should have a perfect diffuse surface and perfect monochromaticity, like Labsphere Spectralon® diffuse color standards. In our experiments, however, the diffuse bases were made of wood coated with matt acrylic paint (Liquitex® soft body), and they showed some specular reflection, multiple color components and light absorption. Besides, the transparent bases were made of acrylic resin tinged with a dye, and they also did not have perfect monochromaticity. Accordingly, we measured the actual color and investigated the color gamut with these RGB bases, as shown in Fig. 15 (h) and (i). Regarding the influence of the specular reflection in diffuse base materials, see the next subsection. Additionally, we also prepared the key material as shown in Fig. 15 (g). Ideally, it also should have perfect light absorption characteristics, like Vantablack [Theocharous et al. 2012]; however, we used a black velvet ball whose reflectance was a few percent.

The results of the color composition are shown in the upper two rows in Fig. 18. Though the base materials were not the best in the prototype, the composition principle and normalization with the key material worked as predicted, and the colors of diffuse and transparent target materials were varied.

5.3 Roughness Reproduction Gamut

To achieve a good approximation of the target roughness, we prepared the base materials with reference to the optimum solution described in section 4.2, as shown in Fig. 16 (a) ~ (c). The base materials in the figures (a) and (b) were made of stainless steel and were processed by sandblasting with about 60 [μm] grit-size glass

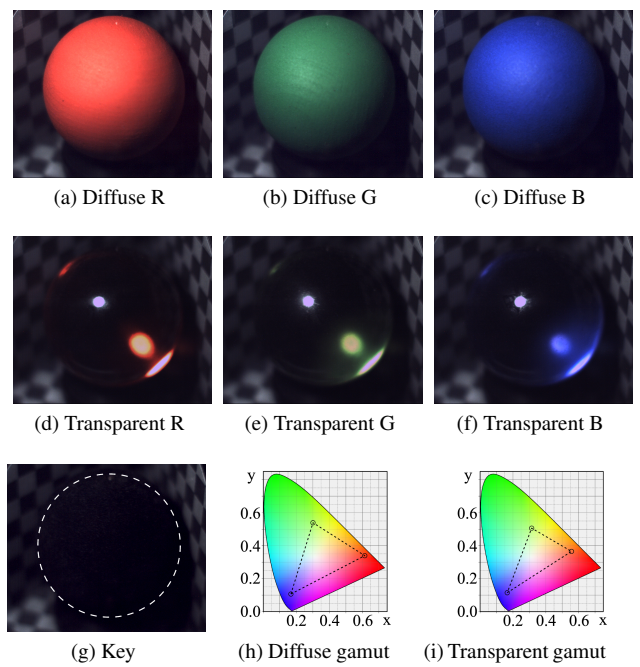


Figure 15: The base materials for the color composition. We prepared diffuse, transparent and key materials. Because prepared objects have incomplete monochromaticity and reflectivity, the color gamuts are not the best.

beads, which was the small available one in our development. We made many glossy balls with different roughnesses by changing the sandblasting time and chose the set of samples with the closest roughnesses. In addition, the base material in (c) was made of wood coated with silver acrylic paint. The roughnesses of the base materials in the prototype were 0.06, 0.15, and 0.48 in the GGX model, and we recalculated the optimal weights for the case of the available bases. In the recalculation, specular reflections in the diffuse base materials were considered, and the BRDFs from which these reflections are subtracted can be used in the MILP problem described in subsection 4.2. However, this recalculation is not required if the ideal base materials are available, and various ideal bases should become available as a result of recent manufacturing technologies [Weyrich et al. 2009][Hašan et al. 2010]. Figure 16 (d) ~ (h) show the error amount, the weights for the best approximation, and the difference in the image at the roughness with the maximum error of all compositions using multiple base materials. In the end, the sum of error is 4.1 [%] higher than in the optimum case.

The results of the roughness composition are shown in the third and fourth rows in Fig. 18. A variety of roughnesses are approximated with only three bases, and the figures show that the composition of diffuse and specular reflections also worked well.

5.4 Reproduction of an Augmented Material and a Spatially-Varying Material

As an example of heterogeneous composition, the left side of the fifth row in Fig. 18 shows the composition of a transparent and diffuse material, a velvety and sharp-specular-reflection material, and a transparent and dull-specular-reflection material. In addition, the right side of the fifth row in the figure shows alpha composition with different alpha values. The sixth row in the figure shows

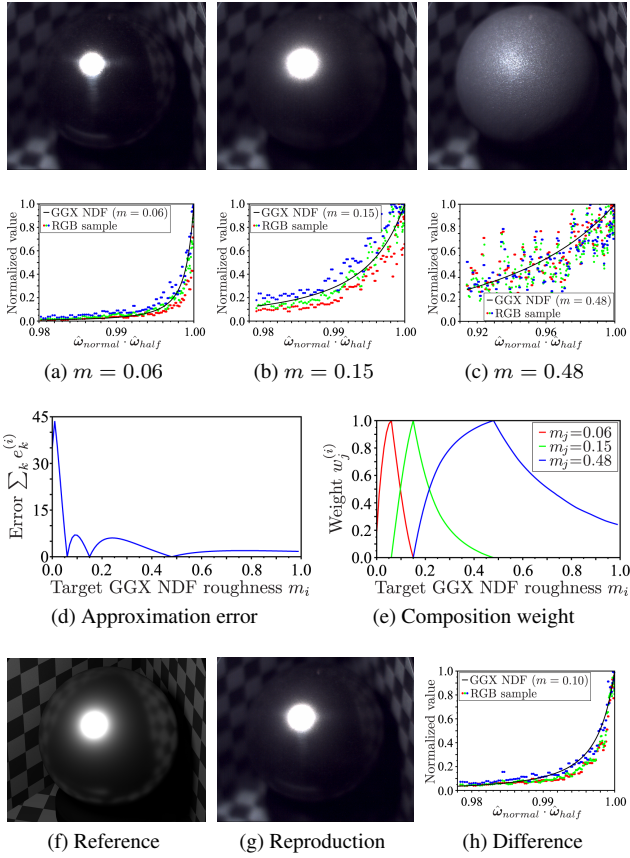


Figure 16: The base materials for roughness composition. Prepared objects used in the experiment had incomplete BRDF due to their mesoscopic roughness, and the measured roughness m did not match the optimal solution exactly. The reproduction with $m = 0.10$, which had the greatest error of all compositions using multiple base materials, shows the worst case with these bases. The reference (f) is an image rendered by computer graphics.

a light-source-dependent material which looks glossy red with the left-side light but looks matt blue with the right-side light. The augmented materials are also expressed with high quality and are seamlessly animated from ordinary materials. This will allow ZoeMatrope to create new physical media, which will be useful in applications such as art, advertising, entertainment, and augmented reality.

The lowest two rows in the figure show a spatially-varying material and maps of the quantities of light. In this experiment, we used a high-speed grayscale projector and specific bit planes in the images as the strobe light in order to keep the exposure time within 92 [μs]. As a result, we realized the presentation of a spatially-varying material with a maximum blur of 1 [mm] at 20 [Hz], though it has only four gradations on each base material. Nevertheless, the performance will be improved in the future. In the configuration with the projector, the texture maps were rasterized, and the resolution was limited by the resolution of the projector; however, within a each texel, the display has the highest resolution, equivalent to that of the real world. Furthermore, this problem arising from discretized maps will be solved by using light with a mask pattern as the light source.

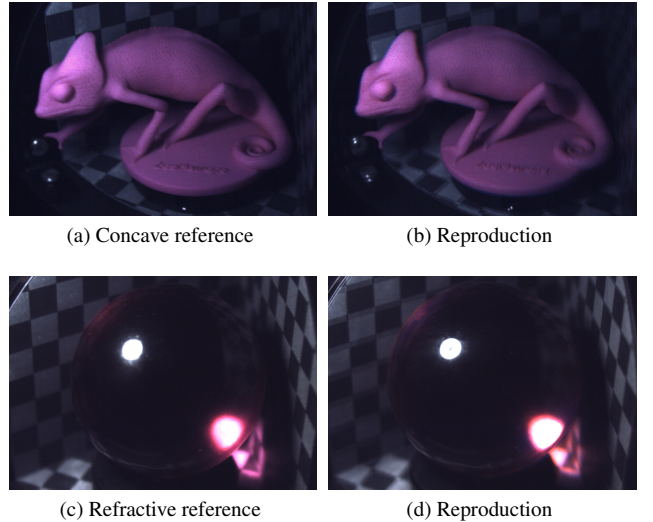


Figure 17: The influence on the appearance in concave and refractive composition. The concave and refractive reproductions were composited with $(R, G, B) = (0.49, 0.51, 0.0)$, $(0.58, 0.42, 0.0)$ bases respectively.

5.5 Limitations of the System

The limitations in the approximation of some parameters such as IOR was mentioned in the subsection 4.3. In this subsection, we focus on the other limitations.

The material representation in our system is determined by the controlled strobe light so uncontrolled ambient light influences the representation quality. However, when the strobe light is bright enough, the effect is not so noticeable as shown in Fig. 1 left. In the figure, the system was affected by a LCD and the light through a window. Besides, the composition principle cannot reproduce a concave or refractive object precisely. In order to evaluate the influence on the appearance in the composition of a concave object, we prepared the concave base materials and the reference object by using 3D printing as shown in the upper row in Fig. 17. Similarly, we prepared a purplish acrylic object as the reference and evaluated the case of the composition of a refractive object as shown in the lower row in Fig. 17. The effect of multi-bounce on the concave object seems slight but the caustics on the reproduction of the refractive object is brighter than the reference. However, the bases also did not have a perfect monochromativity and reflectance or transmittance, so the result will be improved with the ideal bases.

6 Conclusions and Future Work

In this paper, we introduced the ZoeMatrope system which enables realistic display and physical animation of a numerical material in computer graphics. In order to optimally reproduce the target materials, we proposed composition and base selection methods and computationally handled real objects based on the principles of the zoetrope and the thaumatrope. These mathematical frameworks are applicable to most parameters used in computer graphics. As a result, the ZoeMatrope successfully displayed a wide range of materials with a high resolution, wide dynamic range, and good light field reproducibility. We also demonstrated the validity of the methods by compositing materials with the developed system and evaluated the gamut of the materials. Although the base materials available in the prototype were not ideal, they allowed high-quality repro-

duction and showed the potential of the ZoeMatrope. Moreover, the ZoeMatrope can also realize augmented materials, and this will enhance not only material editing but also representation of new materials that will be attractive in various fields, including art, entertainment, and advertising.

Future work will include refinement of the base materials, improved gradation of spatially-varying materials, and a touchable system setup. Ideal base materials can be made available by material manufacturers. Also the projector will be accelerated as high-speed cameras and high-speed image processing technology improve and will perform fast enough to achieve blurless images in the future. In addition, touching is not the focus of the ZoeMatrope, which is a visual display device, but the fusion of visual displays and haptic displays will surely lead to more immersive experiences and interfaces.

References

- BLACKWELL, H. R. 1946. Contrast thresholds of the human eye. *J. Opt. Soc. Am.* 36, 11, 624–643.
- GLASNER, D., ZICKLER, T., AND LEVIN, A. 2014. A reflectance display. *ACM Trans. Graph.* 33, 4, 61:1–61:12.
- HAŠAN, M., FUCHS, M., MATUSIK, W., PFISTER, H., AND RUSINKIEWICZ, S. 2010. Physical reproduction of materials with specified subsurface scattering. *ACM Trans. Graph.* 29, 3, 61:1–61:10.
- HECHT, S., AND SMITH, E. L. 1936. Intermittent stimulation by light vi. area and the relation between critical frequency and intensity. *J. Gen. Physiol.* 19, 6, 979–989.
- HULLIN, M. B., LENSCHE, H. P. A., RASKAR, R., SEIDEL, H.-P., AND IHRKE, I. 2011. Dynamic display of BRDFs. *Computer Graphics Forum* 30, 2, 475–483.
- HULLIN, M. B., IHRKE, I., HEIDRICH, W., WEYRICH, T., DAMBERG, G., AND FUCHS, M. 2013. Computational fabrication and display of material appearance. *Eurographics State-of-the-Art Reports (STAR)*, 137–153.
- JONES, A., McDOWALL, I., YAMADA, H., BOLAS, M., AND DEBEVEC, P. 2007. Rendering for an interactive 360° light field display. *ACM Trans. Graph.* 26, 3, 40:1–40:10.
- JONES, A., NAGANO, K., LIU, J., BUSCH, J., YU, X., AND BOLAS, M. 2014. Interpolating vertical parallax for an autostereoscopic three-dimensional projector array. *J. Electron. Imaging* 23, 1, 011005–1–011005:12.
- KAUTZ, J., AND MCCOOL, M. D. 2000. Approximation of glossy reflection with prefiltered environment maps. In *Proceedings of the Graphics Interface*, (GI ’00), 119–126.
- MATUSIK, W., AJDIN, B., GU, J., LAWRENCE, J., LENSCHE, H. P. A., PELLACINI, F., AND RUSINKIEWICZ, S. 2009. Printing spatially-varying reflectance. *ACM Trans. Graph.* 28, 5, 128:1–128:9.
- NAYAR, S. K., BELHUMEUR, P. N., AND BOULT, T. E. 2004. Lighting sensitive display. *ACM Trans. Graph.* 23, 4, 963–979.
- OCHIAI, Y., AND TAKAI, H. 2011. The cyclone display: Rotation, reflection, flicker and recognition combined to the pixels. In *Proceedings of the 38th Annual Conference on Computer Graphics and Interactive Techniques, Emerging Technologies*, (SIGGRAPH ’11), 16:1–16:1.
- OCHIAI, Y., OYAMA, A., AND TOYOSHIMA, K. 2012. A colloidal display: Membrane screen that combines transparency, BRDF and 3D volume. In *Proceedings of the 39th Annual Conference on Computer Graphics and Interactive Techniques, Emerging Technologies*, (SIGGRAPH ’12), 2:1–2:1.
- RASKAR, R., WELCH, G., LOW, K.-L., AND BANDYOPADHYAY, D. 2001. Shader lamps: Animating real objects with image-based illumination. In *Proceedings of the 12th Eurographics Workshop on Rendering Techniques*, 89–102.
- REN, P., WANG, J., SNYDER, J., TONG, X., AND GUO, B. 2011. Pocket reflectometry. *ACM Trans. Graph.* 30, 4, 45:1–45:10.
- SMOOT, L., BASSETT, K., HART, S., BURMAN, D., AND ROMRELL, A. 2010. An interactive zoetrope for the animation of solid figurines and holographic projections. In *Proceedings of the 37th Annual Conference on Computer Graphics and Interactive Techniques, Emerging Technologies*, (SIGGRAPH ’10), 6:1–6:1.
- THEOCHAROUS, S., THEOCHAROUS, E., AND LEHMAN, J. 2012. The evaluation of the performance of two pyroelectric detectors with vertically aligned multi-walled carbon nanotube coatings. *Infrared Physics and Technology* 55, 4, 299–305.
- WALTER, B., MARSCHNER, S. R., LI, H., AND TORRANCE, K. E. 2007. Microfacet models for refraction through rough surfaces. In *Proceedings of the 18th Eurographics Conference on Rendering Techniques*, (EGSR’07), 195–206.
- WATANABE, Y., NARITA, G., TATSUNO, S., YUASA, T., SUMINO, K., AND ISHIKAWA, M. 2015. High-speed 8-bit image projector at 1,000 fps with 3 ms delay. In *Proceedings of the International Display Workshops*, (IDW ’15), 1064–1065.
- WEYRICH, T., PEERS, P., MATUSIK, W., AND RUSINKIEWICZ, S. 2009. Fabricating microgeometry for custom surface reflectance. *ACM Trans. Graph.* 28, 3, 32:1–32:6.

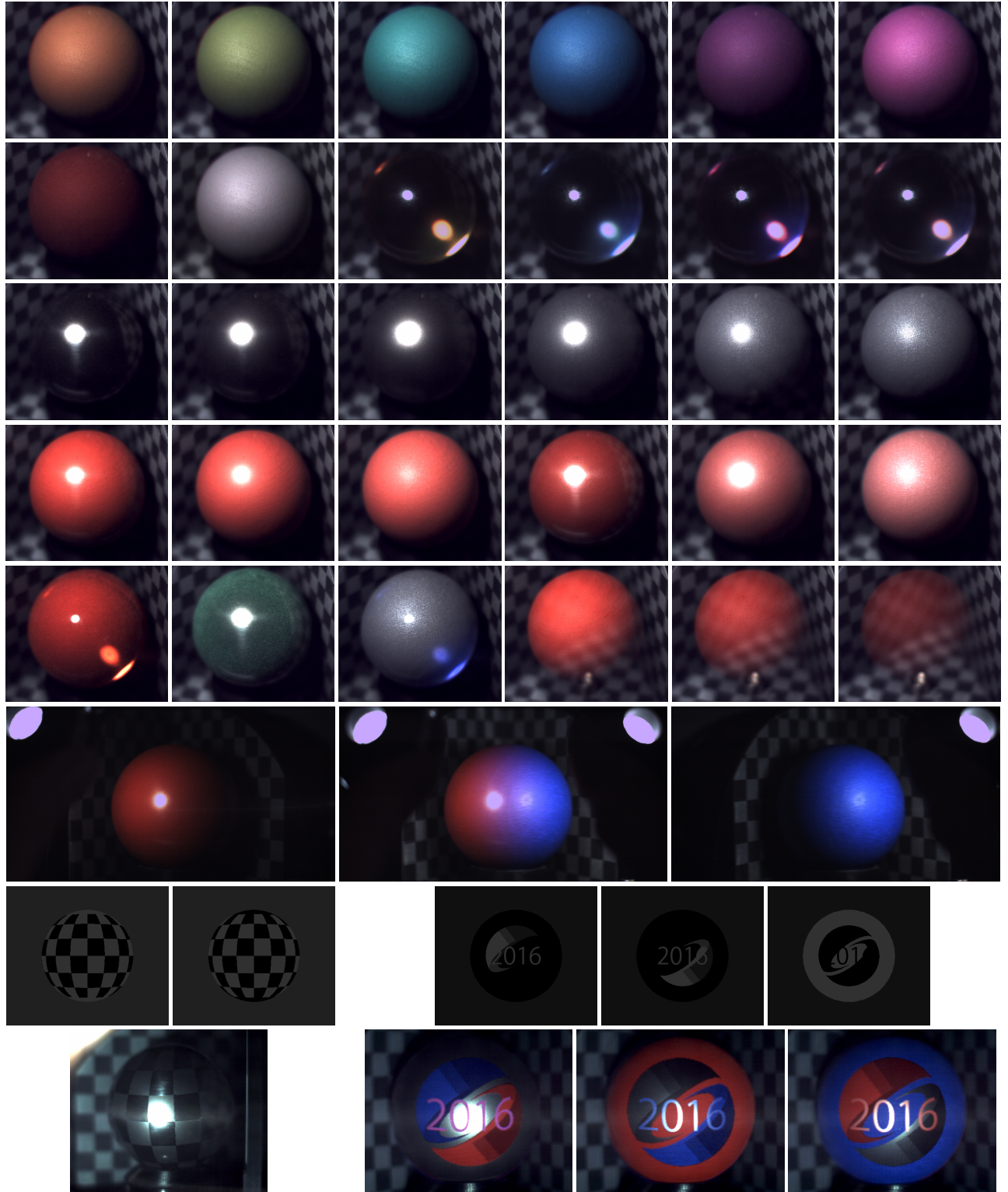


Figure 18: The expressed materials. First row: compositions of diffuse color. Left to right, $(R, G, B) = (1.0, 0.5, 0.0), (0.5, 1.0, 0.0), (0.0, 1.0, 0.5), (0.0, 0.5, 1.0), (0.5, 0.0, 1.0), (1.0, 0.0, 0.5)$. Second row: compositions of dark color, grayscale and transparent color. Left to right, $(R, G, B) = (0.25, 0.0, 0.0), (1.0, 1.0, 1.0), (1.0, 1.0, 0.0), (0.0, 1.0, 1.0), (1.0, 0.0, 1.0), (1.0, 1.0, 1.0)$. Third row: composition of specular roughness. Left to right, $m = 0.05, 0.10, 0.15, 0.20, 0.30, 0.40$. Fourth row: composition of red diffuse and specular reflection. Left to right, $(\alpha, \beta, m) = (0.8, 0.2, 0.05), (0.8, 0.2, 0.20), (0.8, 0.2, 0.40), (0.5, 0.5, 0.05), (0.5, 0.5, 0.20), (0.5, 0.5, 0.40)$. Fifth row: heterogeneous and alpha composition. Left to right, velvet with refraction, velvet with sharp specular reflection, dull reflection with sharp refraction and red diffuse with alpha = 0.75, 0.50, 0.25. Sixth row: light-source-dependent material. Last two rows: composition of spatially-varying material and maps of the quantity of light. Left figures show checkered roughness. Right figures show the siggraph logo in multiple colors and roughnesses.